Online Appendix for 'The Persistent Widening of Cross-Currency Basis: When Increased FX Swap Demand Meets Limits of Arbitrage'

Nadav Ben Zeev*
Ben-Gurion University of the Negev

Daniel Nathan†
University of Pennsylvania and Bank of Israel

July 24, 2023

Abstract

This online appendix consists of the following two appendices: an appendix detailing the Bayesian estimation procedure for the econometric model and an appendix presenting results from robustness checks for the latter model's baseline analysis.

*Department of Economics, Ben-Gurion University of the Negev, Beer-Sheva, Israel. *E-mail:* nadavbz@bgu.ac.il.

†Finance Department, The Wharton School, University of Pennsylvania, Philadelphia, United States, and the Research Department, Bank of Israel, Jerusalem, Israel. *E-mail:* nathad@wharton.upenn.edu.

Appendix A Posterior Distribution of Parameters

Given the block-recursiveness of the econometric model (Equations (14) and (15) from the text), we present the estimation algorithm separately for these two equations.

A.1 Equation (14)

Companion Form of Specification. Keeping with the notation from Section 5.2.1 of the paper, Equation (14) from the text can be written in companion form as follows:

$$Y_i = X_i B_i + \Gamma_i, \tag{A.1}$$

where i indexes IIs and $Y_i = [\Delta SP_{i,1}, ..., \Delta SP_{i,T}]'$, $X = [X_{i,1}, ..., X_{i,T}]'$, $X_{i,t} = [1, ..., Z_{i,t-p_i}]'$, $B = [\alpha_{i,0,L}, ..., C_{i,p_i}]'$, and $\Gamma_i = [\epsilon_{i,1}, ..., \epsilon_{i,T}]'$ (with T being the time dimension of the sample and p_i being the number of lags). B_i here represents the reduced form coefficient vector of Equation (14) from the text and $\sigma^2_{i,\epsilon}$ is the variance of the reduced form innovation series $\epsilon_{i,t}$ from that equation.

Specification of Uninformative Prior. We follow the conventional approach of specifying a normal-inverse Wishart prior distribution for the reduced-form parameters:[1]

$$vec(B_i) \mid \sigma^2_{i,\epsilon} \sim N(vec(\bar{B}_0), \sigma^2_{i,\epsilon} \otimes N_0^{-1}), \tag{A.2}$$

$$\sigma^2_{i,\epsilon} \sim IW_1(v_0 S_0, v_0), \tag{A.3}$$

where N_0 is a KxK positive definite matrix (K is the number of parameters for the RHS of Equation (14)), S_0 is a scalar, and $v_o > 0$. As shown by Uhlig (1994), the latter prior implies the following posterior distribution:

$$vec(B_i) \mid \sigma^2_{i,\epsilon} \sim N(vec(\bar{B}_{i,T}), \sigma^2_{i,\epsilon} \otimes N_{i,T}^{-1}), \tag{A.4}$$

$$\sigma^2_{i,\epsilon} \sim IW_1(v_T S_{i,T}, v_T), \tag{A.5}$$

where $v_T = T + v_0$, $N_{i,T} = N_0 + X_i' X_i$, $\bar{B}_{i,T} = N_{i,T}^{-1}(N_0 \bar{B}_0 + X_i' X_i \hat{B}_i)$,
$S_{i,T} = \frac{v_0}{v_T} S_0 + \frac{T}{v_T} \hat{\sigma^2_{i,\epsilon}} + \frac{1}{v_T}(\hat{B}_I - \bar{B}_0)' N_0 N_{i,T}^{-1} X_i' X_i (\hat{B}_i - \bar{B}_0)$, $\hat{B}_i = (X_i' X_i)^{-1} X_i' Y_i$,
and $\hat{\sigma^2_{i,\epsilon}} = (Y_i - X_i \hat{B}_i)'(Y_i - X_i \hat{B}_i)/T$.

[1] Since Equation (14) from the text is univariate, the assumed inverse-Wishart distribution for σ^2_ϵ is denoted by IW_1, where the subscript 1 represents the univariate nature of Equation (14) from the text and its corresponding univariate inverse-Wishart distribution.

We follow the literature and use a weak prior, i.e., $v_0 = 0$, $N_0 = 0$, and arbitrary S_0 and $\bar{B}_0$. This implies that the prior distribution is proportional to $\sigma^2_{i,\epsilon}$ and that $v_T = T$, $S_{i,T} = \hat{\sigma^2_{i,\epsilon}}$, $\bar{B}_{i,T} = \hat{B}_i$, and $N_{i,T} = X_i'X_i$.

Posterior Simulator. In light of the above-described prior formulation, the posterior simulator for B_i and $\sigma^2_{i,\epsilon}$ can be described as follows:

1. Draw $\sigma^2_{i,\epsilon}$ from an $IW_1(T\hat{\sigma^2_{i,\epsilon}}, T)$ distribution.
2. Draw B_i from the conditional distribution $MN(\hat{B}_i, \sigma^2_{i,\epsilon} \otimes (X_i'X_i)^{-1})$.
3. Repeat steps 1 and 2 a large number of times and collect the drawn B_i's and $\sigma^2_{i,\epsilon}$'s.[2]

Once we have these draws at hand, we compute the standardized aggregate shock to IIs' FX swap demand (i.e., our granular instrumental variable (GIV) shock), which is the difference between the size-weighted- and inverse-variance-weighted average of the II-specific residuals from Equation (14) from the text divided by the standard deviation of this difference, and feed it into the estimation of Equation (15) from the text, as described next.

A.2 Equation (15)

Companion Form of Specification. Drawing on the notation from Section 5.2.1 of the paper, let the set of the parameters (coefficients matrix and residual standard deviation) to be estimated from Equation (15) from the text be given by Q_h and $\sigma_{u,h}$. Equation (8) from the text can then be written in companion form as follows:[3]

$$Y_h = X_h Q_h + \zeta_h, \tag{A.6}$$

where h is the regression's rolling horizon with $h = 0, ..., 600$; $Y_h = [b_h - b_{-1}, b_{h+1} - b_0, ..., b_T - b_{T-h-1}]'$; $X_h = [X_1, ..., X_{T-h}]'$, with $X_t = [1, ..., LOA_{t-1}\hat{\varepsilon}_t]'$; $Q_h = [\alpha_{2,L,h}, ..., \Xi_{I,h}]'$; and $\zeta_h = [u_h, ..., u_T]'$.

[2] We generate 500 such posterior draws.

[3] While there is, technically speaking, notational abuse of capital letters Y and X in Equations (A.1) and (A.6), what matters is that they are of course defined and used in the context of their corresponding equations and hence their specific contexts avoid expositional confusion. (The context for the first equation is a single equation while for the second it is a rolling regression context (hence the use of subscript h for Y in the second equation).)

Q_h here represents the coefficient matrix of Equation (15) from the text and $\sigma^2_{u,h}$ is the variance of u_{t+h} (the residual from that equation).

Specification of Uninformative Prior. We assume the following normal-inverse Wishart prior distribution for these parameters:

$$vec(Q_h) \mid \sigma^2_{u,h} \sim N(vec(\bar{Q}_{0,h}), \sigma^2_{u,h} \times N_0^{-1}), \tag{A.7}$$

$$\sigma^2_{u,h} \sim IW_1(v_0 S_{0,h}, v_0), \tag{A.8}$$

where N_0 is a 2 x 2 positive definite matrix; S_0 is a variance scalar; and $v_o > 0$. As shown by Uhlig (1994), the latter prior implies the following posterior distribution:

$$vec(Q_h) \mid \sigma^2_{u,h} \sim N(vec(\bar{Q}_h), \sigma^2_{u,h} \times N_h^{-1}), \tag{A.9}$$

$$\sigma^2_{u,h} \sim IW_1(v_h S_h, v_h), \tag{A.10}$$

where $v_h = T - h + v_0$; $N_h = N_0 + X_h' X_h$; $\bar{Q}_h = N_h^{-1}(N_0 \bar{Q}_{0,h} + X_h' X_h \hat{Q}_h)$; $S_h = \frac{v_0}{v} S_{0,h} + \frac{T-h+1}{v_h}\hat{\sigma}^2_{u,h} + \frac{1}{v_h}(\hat{Q}_h - \bar{Q}_{0,h})' N_0 N_h^{-1} X_h' X_h (\hat{Q}_h - \bar{Q}_{0,h})$, where $\hat{Q}_h = (X_h' X_h)^{-1} (X_h)' Y$ and $\hat{\sigma}^2_{u,h} = (Y_h - X_h \hat{Q}_h)'(Y_h - X_h \hat{Q}_h)/(T-h)$.

We use a weak prior, i.e., $v_0 = 0$, $N_0 = 0$, and arbitrary $S_{0,h}$ and $\bar{Q}_{0,h}$. This implies that the prior distribution is proportional to $\sigma^2_{u,h}$ and that $v_h = I \times (T-h)$, $S_h = \hat{\sigma}^2_{u,h}$, $\bar{Q}_h = \hat{Q}_h$, and $N_h = X_h' X_h$. Due to the temporal correlations of the error term ϵ_{t+h}, the likelihood function is misspecified which in turn requires that the residual variance estimate $\hat{\sigma}^2_{u,h}$ be appropriately modified so as to improve estimation precision (Müller (2013)). Toward this end, we apply a Newey-West correction to $\hat{\sigma}^2_{u,h}$ which accounts for arbitrary temporal correlation of the error term and denote the corrected variance estimate by $\hat{\sigma}^2_{u,h,hac}$.

Posterior Simulator. Given the above-described prior formulation and the correction to $\hat{\sigma}^2_{u,h}$, we are now in position to lay out the posterior simulator for Q_h and $\sigma^2_{u,h}$, which accounts for uncertainty in the estimation of the aggregate FX swap demand shock series $\hat{\epsilon}_t$ and can be described as follows:

1. Do Steps 1-3 from the posterior simulator of Equation (14) from the text and obtain $\hat{\epsilon}_t$ (whose standardized value is to be used as explanatory variables for the next two steps).

2. Draw $\sigma^2_{u,h}$ from an $IW_1((T-h+1)\hat{\sigma}^2_{u,h,hac}, (T-h+1))$ distribution.

3. Draw Q_h from the conditional distribution $MN(\hat{Q}_h, \sigma^2_{u,h} \times (X_h' X_h)^{-1})$.

4. Repeat Steps 1-3 a large number of times and collect the drawn Q_h's and $\sigma^2_{u,h}$'s.[4]

A.3 Smoothing of Impulse Responses

The high-frequency nature of our data combined with our local projection estimation approach produce rather jagged raw impulse responses. It is therefore important and warranted to smooth the raw impulse responses with a data-dependent smoothing procedure that suitably integrates into our Bayesian framework. We now turn to present this procedure.

General Setting and Objective. Let $\Theta_L = [\Xi_{L,1}, \Xi_{L,2}, ..., \Xi_{L,500}]'$ and $\Theta_I = [\Xi_{I,1}, \Xi_{I,2}, ..., \Xi_{I,500}]'$ denote the raw linear and non-linear (interaction term based) impulse response 500×1 vectors, respectively. The posterior simulator of Steps 1-4 shows how to obtain posterior draws for these vector and hence effectively gives knowledge of its posterior probability distribution $\mathbb{P}(\Theta_j \mid data)$ ($j = [L, I]$). We assume the following smooth trend, state-space model for $\Xi_{j,h}$ (with h representing the horizon and $j = [L, I]$):

$$\Xi_{j,h} = \tilde{\Xi}_{j,h} + \eta_{j,h}, \tag{A.11}$$

$$\tilde{\Xi}_{j,h} = 2\tilde{\Xi}_{j,h-1} - \tilde{\Xi}_{j,h-2} + \gamma_{j,h}, \tag{A.12}$$

where Equation (A.11) is the model's measurement equation and Equation (A.12) is the model's state equation; $\tilde{\Xi}_{j,h}$ is the smoothed impulse response at horizon h whose first-difference follows a random walk with shock $\gamma_{j,h}$, which is a zero-mean independently and identically normally distributed variable with variance σ_γ; and $\eta_{j,h}$ is a zero-mean independently and identically normally distributed variable with variance σ_η which represents the noise embodied in the raw impulse response function (IRF). Letting $\tilde{\Theta}_j = [\tilde{\Xi}_{j,1}, \tilde{\Xi}_{j,2}, ..., \tilde{\Xi}_{j,500}]'$ denote the smoothed impulse response 500×1 vector, our main interest and objective can be described as lying in simulating $\tilde{\Theta}_j$ from its posterior probability distribution $\mathbb{P}(\tilde{\Theta}_j \mid data)$.

[4]The number of posterior draws is 500, as this posterior simulator generates a posterior draw for each of the 500 drawn FX swap demand shocks from the estimation of Equation (14).

Relation of Model (A.11)-(A.12) to HP-Filter. The smooth trend, state-space model from Equations (A.11)-(A.12) can be viewed as a model-based interpretation of Hodrick and Prescott (1997)'s popular HP-filter (see, e.g., Harvey (1990), Gómez (1999), and Appendix D from Cornea-Madeira (2017)). Specifically, the MSE-optimal smoothed $\tilde{\Xi}_h$ obtained from applying the Kalman filter to this model to find the values for σ_η and σ_γ that maximize the likelihood function for Θ_j ($\mathbb{P}(\Theta_j \mid \sigma_\eta, \sigma_\gamma, data)$) corresponds to the HP-filter of $\Xi_{j,h}$ with smoothing parameter $\frac{\sigma_\eta^2}{\sigma_\gamma^2}$.[5] In this sense, the way we model the smoothed IRF follows the general suggestion from Plagborg-Møller (2016) to smooth raw impulse responses with the HP-filter.[6]

Treatment of Hyperparamters σ_η and σ_γ. To simulate posterior draws of $\tilde{\Theta}_j$, we need to simulate posterior draws from the joint posterior probability distribution of Θ_j, σ_η, and σ_γ, $\mathbb{P}(\Theta_j, \sigma_\eta, \sigma_\gamma \mid data)$, and then use the Kalman filter smoother to obtain posterior draws of $\tilde{\Theta}_j$. Bayes' law dictates that $\mathbb{P}(\Theta_j, \sigma_\eta, \sigma_\gamma \mid data) = \mathbb{P}(\sigma_\eta, \sigma_\gamma \mid \Theta_j, data)\mathbb{P}(\Theta_j \mid data)$ and that $\mathbb{P}(\sigma_\eta, \sigma_\gamma \mid \Theta_j, data) \propto \mathbb{P}(\Theta_j \mid \sigma_\eta, \sigma_\gamma, data)\mathbb{P}(\sigma_\eta, \sigma_\gamma \mid data)$.

Since we have knowledge of $\mathbb{P}(\Theta_j \mid data)$ from the previous section's estimation, all we need in order simulate posterior draws from $\mathbb{P}(\Theta_j, \sigma_\eta, \sigma_\gamma \mid data)$ is to know $\mathbb{P}(\sigma_\eta, \sigma_\gamma \mid \Theta_j, data)$. Following the approach of Giannone et al. (2015) and Miranda-Agrippino and Ricco (2021), we treat σ_η and

[5] Hamilton (2018) uses this maximum likelihood estimation procedure for several popular macro time series and finds very low values for the smoothing parameter (see his Table 1), which constitutes an important underlying evidence for his criticism against using the HP-filter and the validity of the assumptions that underlie its estimation. However, his criticism pertains to using the HP-filter for *macro time series*, not IRFs. Hence, his work should not be viewed through the lens of an estimation framework seeking to smooth impulse responses. Accordingly, and in contrast to his estimates for macro time series, our estimated posterior distribution for the smoothing parameter for the non-informative prior case is rather tightly centered around very high smoothing parameters.

[6] Plagborg-Møller (2016) puts forward a classical estimation procedure that selects a shrinkage smoothing parameter that minimizes the unbiased risk estimate (URE) object, which was shown by Plagborg-Møller (2016) to be an asymptotically uniformly unbiased estimator of MSE of the smoothed impulse response estimates relative to the raw ones. What is particularly appealing about the HP-filter-based smoothing approach for our setting is that it optimally smoothes an *estimated* impulse response function; hence, we can conveniently use it within our Bayesian estimation framework as explained in this section. Two additional proposed smoothing procedures for local projections that have been recently put forward are Barnichon and Brownlees (2019)'s frequentist B-spline smoothing estimation procedure and Tanaka (2019)'s Bayesian B-spline smoothing estimation procedure; however, both are effectively generalized ridge estimation procedures that are not directly applied to the standard raw estimated impulse responses, thus rendering them void of the HP-filter based appealing feature mentioned above in the context of our Bayesian setting.

σ_γ as additional model parameters for which we specify a bivariate uniform prior probability distribution and estimate them via the Kalman filter as the maximizers of the posterior likelihood $\mathbb{P}(\sigma_\eta, \sigma_\gamma \mid \Theta_j, data)$, in the spirit of hierarchical modeling. Our assumed flat prior for the joint prior distribution of σ_η and σ_γ (conditional on the observed data), $\mathbb{P}(\sigma_\eta, \sigma_\gamma \mid data)$, implies equivalency between maximizing $\mathbb{P}(\Theta_j \mid \sigma_\eta, \sigma_\gamma, data)$ and $\mathbb{P}(\sigma_\eta, \sigma_\gamma \mid \Theta_j, data)$ (with respect to σ_η and σ_γ).

Estimation of $\mathbb{P}(\tilde{\Theta}_j \mid data)$. We are now in position to describe the estimation of the posterior distribution of the smoothed IRF $\tilde{\Theta}_j$. As noted on Page 5, this posterior distribution can be obtained from $\mathbb{P}(\Theta_j, \sigma_\eta, \sigma_\gamma \mid data)$ by using the Kalman filter smoother to produce $\tilde{\Theta}_j$ from the posterior draws of Θ_j, σ_η, and σ_γ.

In particular, for each posterior draw of $\Xi_{j,h}$, we perform an unconstrained Kalman filter estimation of Model (A.11)-(A.12) which provides us with estimates of σ_η and σ_γ that we denote by $\sigma_{\eta,MLE}$ and $\sigma_{\gamma,MLE}$, respectively. This Kalman filter estimation provides us with estimates of σ_η and σ_γ which we then feed into the Kalman filter smoother to produce a smoothed IRF. Applying this smoothing procedure to the 500 posterior draws of raw IRFs results in the sought after posterior distribution of smoothed IRFs.

Appendix B Robustness Checks

This section examines the robustness of the baseline results from the text (presented in Figure 6-8) along three dimensions. (Two additional robustness dimensions, whose results are shown in the text in Sections 6.4 and 6.5, concern looking at the response of the 1-, 3-, and 6-month bases from Thomson Reuters (i.e., market-wide bases) instead of the baseline aggregate IIs' basis and using the Bartik instrument identification approach instead of the GIV-based one.) First, constructing an alternative intermediary leverage ratio variable as our LOA measure instead of the baseline He et al. (2017) one by considering the largest global FX dealers in the USD/NIS FX swap market. Second, excluding the COVID period. And third, altering the lag specifications underlying Equation (14) from the text. The presentation of all of the results follows the same exposition and structure underlying the baseline results from Figures 6-8 from the text.

B.1 Alternative Intermediary Leverage Ratio Variable

He et al. (2017)'s intermediary leverage ratio variable is based on the list of Primary Dealer counterparties of the New York Federal Reserve in its implementation of monetary policy. In particular, He et al. (2017) construct the aggregate leverage ratio for the intermediary sector by matching the New York Fed's primary dealer list with CRSP/Compustat and Datastream data on their publicly traded holding companies (22 in total), resulting in a leverage ratio variable which corresponds to the largest and most sophisticated financial institutions that operate in virtually the entire universe of capital markets.The appealingness of He et al. (2017)'s LOA measure comes from the fact that even if not all of the 22 primary dealers are effectively operating as arbitrageurs in the USD/NIS FX swap market, the arbitrage capital required for such arbitrage activity crucially hinges on the financial health of this broad set of intermediaries.

Nevertheless, it is still of value to confirm that using the leverage ratio for the subset of He et al. (2017)'s group of global intermediaries that is most active in the USD/NIS FX swap market as the LOA measure also produces similar results to the baseline ones. Toward this end, we construct a value-weighted leverage ratio variable for 12 such intermediaries whose activity (transactions' volume) in the USD/NIS FX swap market accounts for 95% of the entire activity of foreign financial institutions. These 12 intermediaries are a subset of He et al. (2017)'s group of intermediaries.[7]

Figures B.1-B.3 present the results from estimation of Equations (14) and (15) from the text where in the former equation we simply replace the baseline He et al. (2017)'s variable with our 12-intermediary-based leverage ratio variable. The message from the baseline results continues to hold also for this specification. There is a significant and persistent cross-currency basis widening in the LOA state conditional on the aggregate FX swap demand shock, with a peak widening of 7.9 basis points after 405 trading days, while the linear (no LOA) case sees no such widening taking place. The FEV results are also similar to the baseline case, with the aggregate FX swap demand shock accounting for a peak FEV share of 63.6% IIs' basis after 538 horizons.

IIs' open FX swap position moves significantly more in the linear case than in the LOA state through the first 102 horizons, which in turn supports the interpretation of our results as being

[7]Specifically, they include BNP; UBS; Deutsche Bank; HSBC; Barclays; Credit Suisse; Societe Generale; Goldman Sachs; JPM; Citigroup; BoFA; and Wells Fargo.

driven by a meaningful LOA-dependent FX swap demand channel. And similar to the baseline case, IIs' FX swap position rises significantly and persistently in the LOA state in later horizons, in line with the persistent response of the basis. (This significance holds continuously from the 12th to 387th horizons.)

B.2 Excluding the COVID-19-Period

While the COVID-19-related period provides increased volatility to our baseline sample and thus has the potential of improving identification of the LOA-dependent FX swap demand channel, one may also argue that its uniqueness makes the case for showing that the baseline results are not driven by its inclusion. Toward this end, Figures B.4-B.6 present the results from truncating the baseline sample at February 28, 2020. These figures follow the same exposition and structure as the baseline figures from the text (Figures 6-8).

The results from Figures B.4-B.6 indicate that the baseline message of the paper does not change from exclusion of the COVID-19-related period. The aggregate FX swap demand shock continues to induce significant and persistent cross-currency basis widening in the LOA state while failing to do so in the no LOA state. The peak widening of the basis takes place after 347 trading days and stands at 10.9 basis points. FEV contributions are similar to the baseline ones, peaking at 77.2% after 507 trading days.

The demand shock moves the IIs' open FX swap position significantly more in the linear case than in the LOA state initially (through the first 43 horizons). At the same time, we continue to observe a significantly persistent position build-up of IIs in the LOA state, with the response significance initializing after 7 trading days and subsiding only after 468 trading days.[8] The initial significantly lower response of the swap position relative to the corresponding linear (no LOA) response, like in the baseline case, supports the interpretation of the results as evidencing a meaningful LOA-dependent channel of FX swap demand.

[8] In later horizons for the linear case, foreign arbitrageurs appear to supply FX swaps in excess of the demand increase coming from IIs which in turn implies that local arbitrageurs are demanding, rather than supplying, dollar swaps in these horizons. It is beyond the scope of this paper to further explore and explain this interesting behavior especially given that the validity of our findings on the presence of a meaningful LOA-dependent FX swap demand channel are independent of the exact quantitative manner by which local and foreign arbitrageurs meet IIs' increased demand.

B.3 Alternative Lags in Micro Regressions

As noted in Footnote 18 from the text, our baseline lag specification for each II-level regression (Equation (14) from the text) was taken as the average of the suggested lags from the AIC, corrected AIC, BIC and HQIC tests. Taking a middle value of these tests seems like a reasonable compromise given the tendency of AIC and HQIC to overfit as well as that of BIC to underfit. Nevertheless, since the suggested lags from HQIC and BIC were actually too low for the micro regressions to produce white noise residuals (i.e., ones that pass the Ljung-Box Q-test for residual autocorrelation), it seems worthwhile to confirm that increasing the number of lags by considering only the corrected-AIC-suggested lag choices for each of our 14 micro regressions does not change our baseline results.[9] Such confirmation is important as it would ensure that our results are not driven by an error in our lag selection.

The results for the corrected AIC alternative lag specification are shown in Figures B.7-B.9 with the exposition and structure underlying these figures being the same as in the corresponding baseline figures from the text (Figures 6-8).

The results from this alternative lag specification are both quantitatively and qualitatively similar to the baseline results. The aggregate FX swap demand shock continues to induce significant and persistent cross-currency basis widening in the LOA state, with peak such widening of 8.1 basis points after 373 horizons, while producing an insignificant basis response in the linear (no LOA) case. FEV contributions are also similar to the baseline ones. And the demand shock moves the IIs' open FX swap position by significantly less initially in the LOA state, further bolstering confidence in the view that a meaningful LOA-dependent channel of FX swap demand is borne out by our data. The delayed significant persistence of the swap position's response in the LOA state is maintained for the considered alternative lag specification and accords with the strong persistence in the response of the basis in this state.

[9] Similar results obtain from using the *uncorrected*-AIC-suggested lag choices.

Figure B.1: **LOA-Dependent Impulse Responses of IIs' Aggregate Cross-Currency Basis to a One Standard Deviation Aggregate FX Swap Demand Shock: Alternative LOA Measure**.

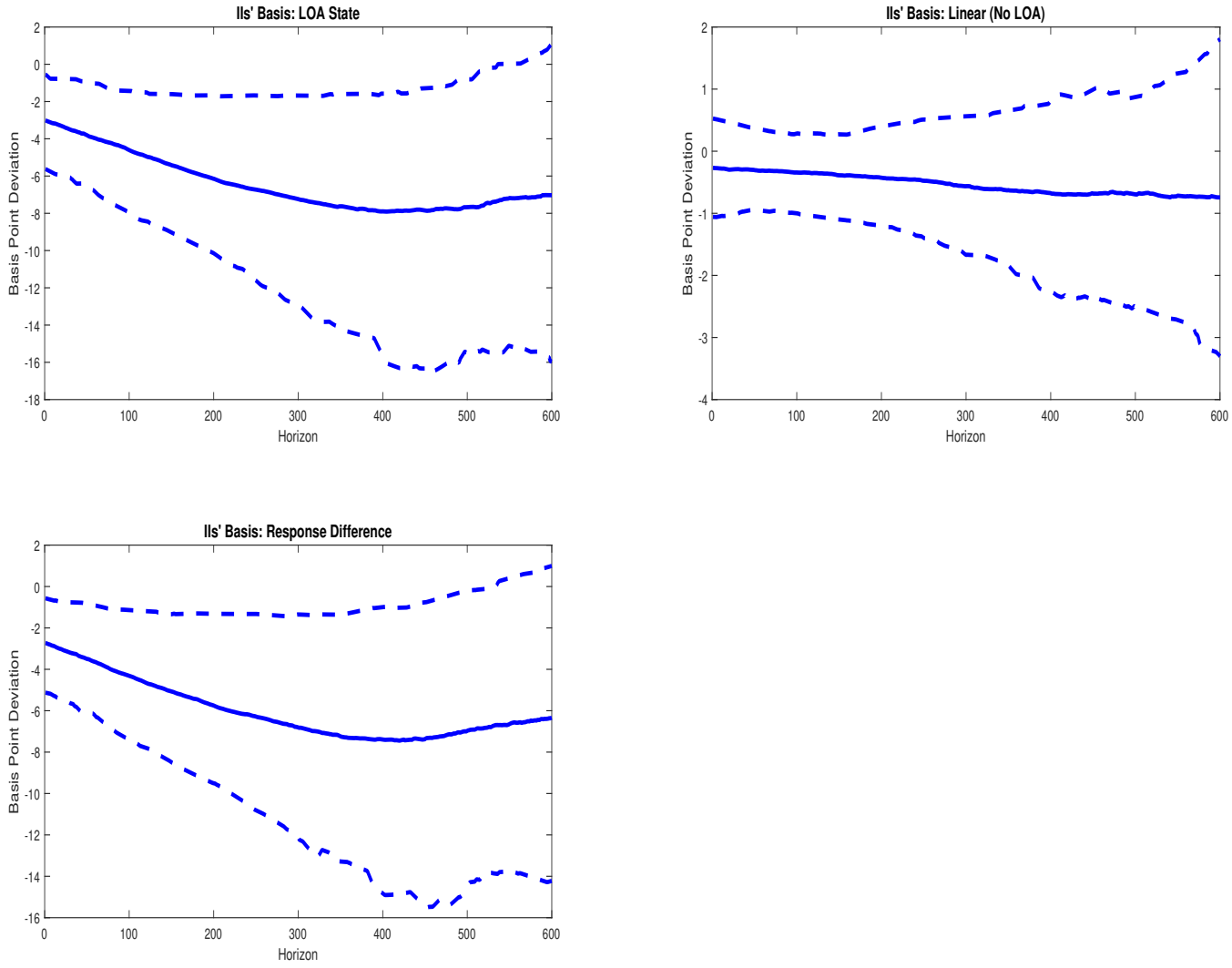

Notes: This figure presents the LOA-dependent impulse responses of IIs' aggregate cross currency basis to a one standard deviation aggregate FX swap demand shock from the model described by Equations (14) and (15) from the text, where now the LOA measure is based on the leverage ratio of the most active global FX dealers in the USD/NIS FX swap market instead of the baseline He et al. (2017)'s intermediary leverage ratio variable. The first and second columns show the responses in the LOA state and linear (no LOA) case, respectively; and the third column shows the response differences across these two cases. Responses are in terms of deviations from pre-shock values (basis point deviations). Horizon (on x-axis) is in days.

Figure B.2: **LOA-Dependent FEV Shares of IIs' Aggregate Cross-Currency Basis Attributable to the Aggregate FX Swap Demand Shock: Alternative LOA Measure**.

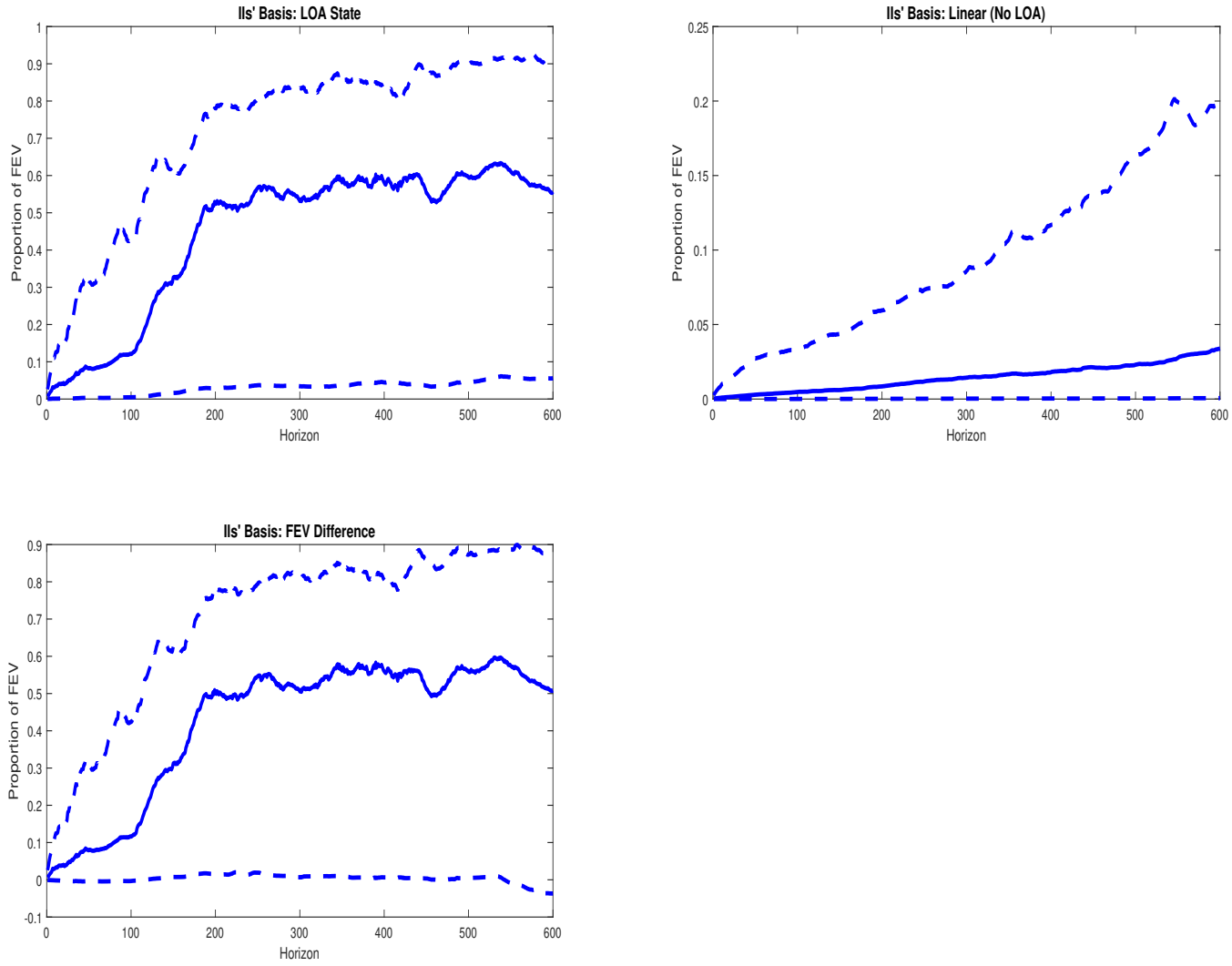

Notes: This figure presents the FEV share of IIs' aggregate cross-currency basis that is attributable to the aggregate FX swap demand shock from the model described by Equations (14) and (15) from the text, where now the LOA measure is based on the leverage ratio of the most active global FX dealers in the USD/NIS FX swap market instead of the baseline He et al. (2017)'s intermediary leverage ratio variable. The first and second columns show the FEV contributions in the LOA state and linear (no LOA) case, respectively; and the third column shows the FEV contribution differences across these two cases. Horizon (on the x-axis) is in days and the FEV share is on the y-axis.

Figure B.3: **LOA-Dependent Impulse Responses of IIs' Aggregate Open FX Swap Position to a One Standard Deviation Aggregate FX Swap Demand Shock: Alternative LOA Measure**.

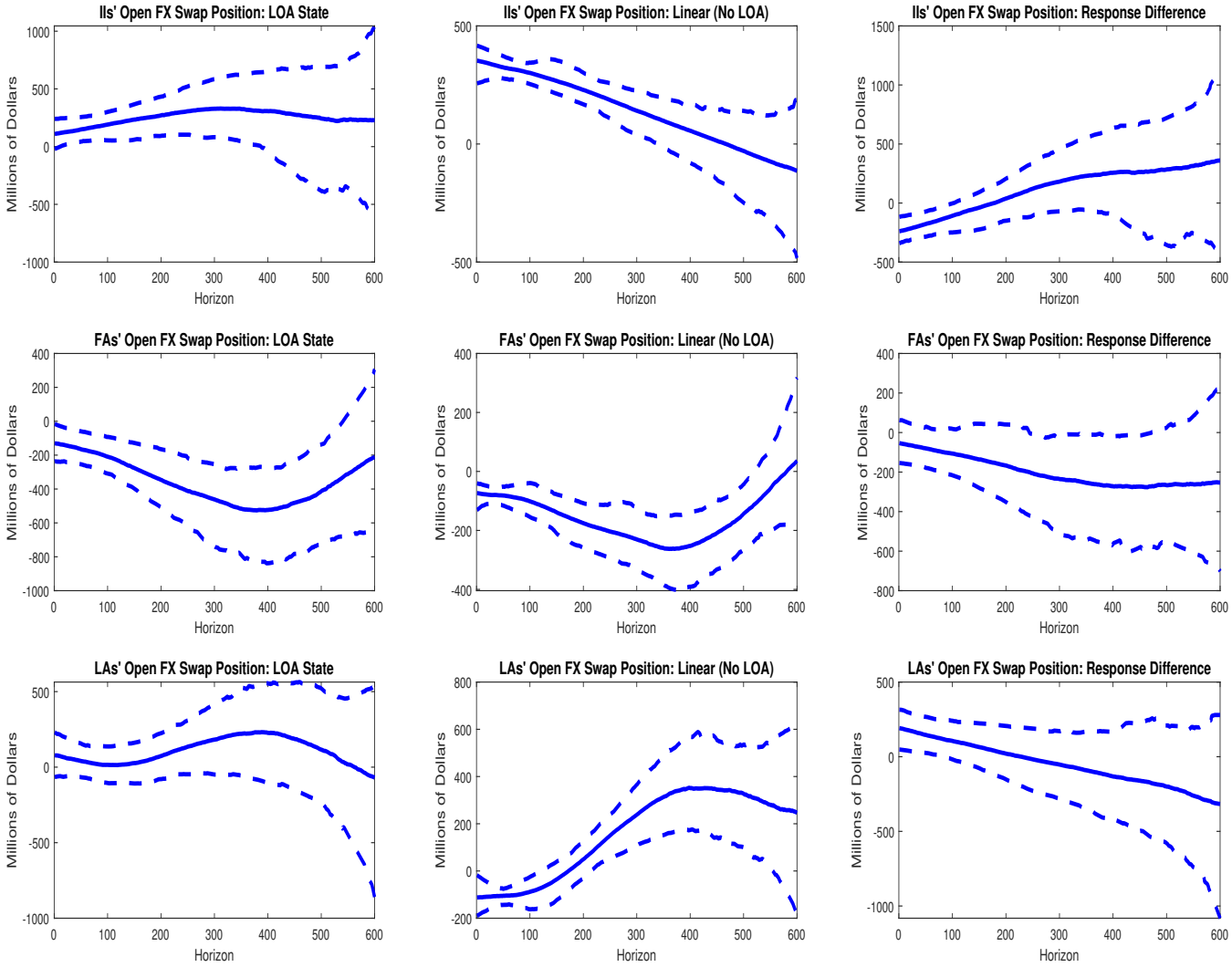

Notes: This figure presents the LOA-dependent impulse responses of IIs', local arbitrageurs' (LAs'), and foreign arbitrageurs' (FAs') aggregate open swap positions to a one standard deviation aggregate FX swap demand shock from the model described by Equations (14) and (15) from the text where the outcome variable in the latter equation (accumulated difference in IIs' basis) is now replaced by the accumulated difference in the corresponding sector's open FX swap position (i.e., $SP_{t+h,j} - SP_{t-1,j}$, where $j = [IIs, LAs, FAs]$). Different from the baseline case, the LOA measure is now based on the leverage ratio of the most active global FX dealers in the USD/NIS FX swap market instead of the He et al. (2017)'s intermediary leverage ratio variable. The first and second columns show the responses in the LOA state and linear (no LOA) case, respectively; and the third column shows the response differences across these two cases. Responses are in terms of deviations from pre-shock values (in millions of dollars terms). Horizon (on x-axis) is in days.

Figure B.4: **LOA-Dependent Impulse Responses of IIs' Aggregate Cross-Currency Basis to a One Standard Deviation Aggregate FX Swap Demand Shock: Excluding COVID**.

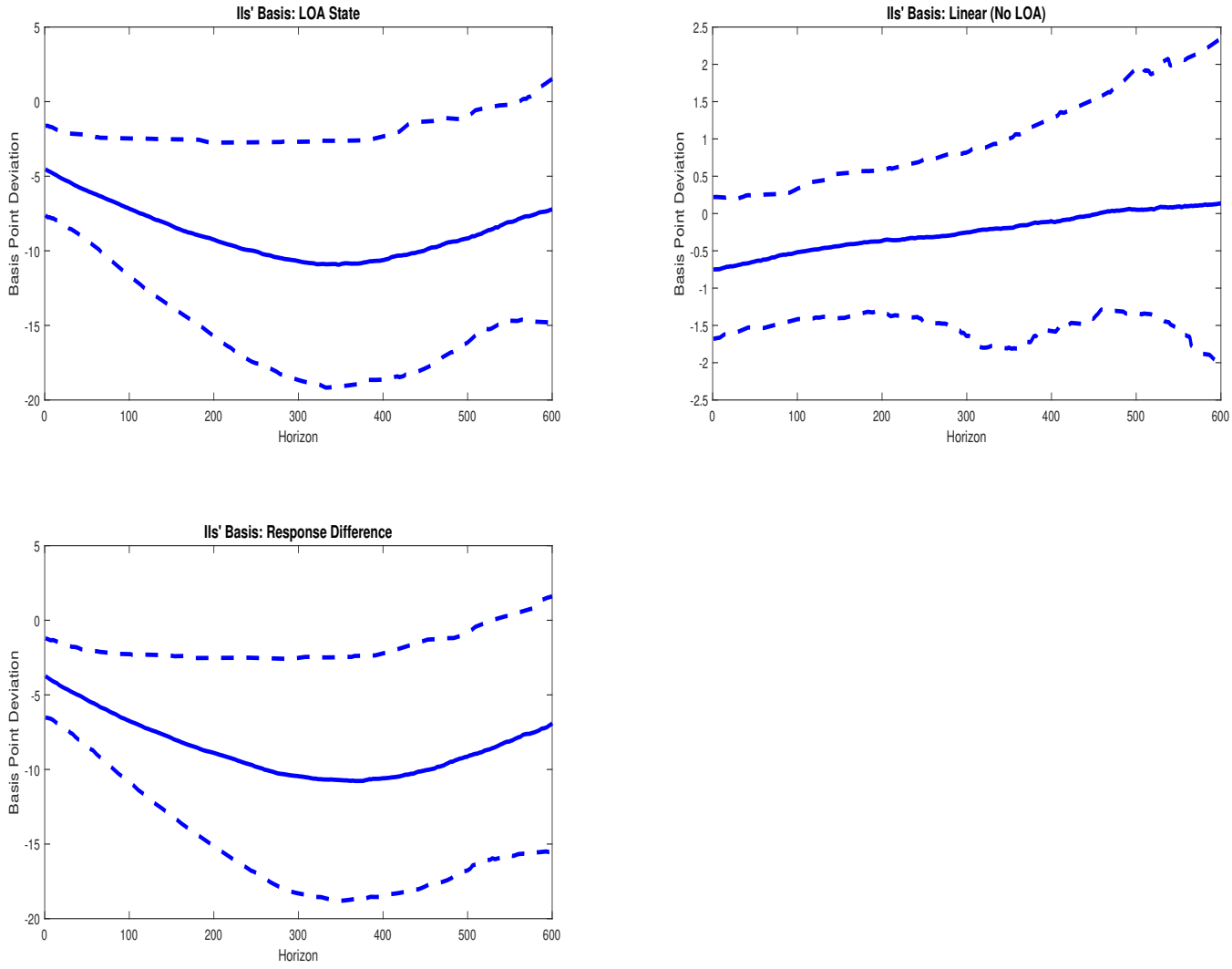

Notes: This figure presents the LOA-dependent impulse responses of IIs' aggregate cross currency basis to a one standard deviation aggregate FX swap demand shock from the model described by Equations (14) and (15) from the text, where now the sample is truncated at February 28, 2020 so as to exclude the COVID-ridden period. The first and second columns show the responses in the LOA state and linear (no LOA) case, respectively; and the third column shows the response differences across these two cases. Responses are in terms of deviations from pre-shock values (basis point deviations). Horizon (on x-axis) is in days.

Figure B.5: **LOA-Dependent FEV Shares of IIs' Aggregate Cross-Currency Basis Attributable to the Aggregate FX Swap Demand Shock: Alternative LOA Measure: Excluding COVID**.

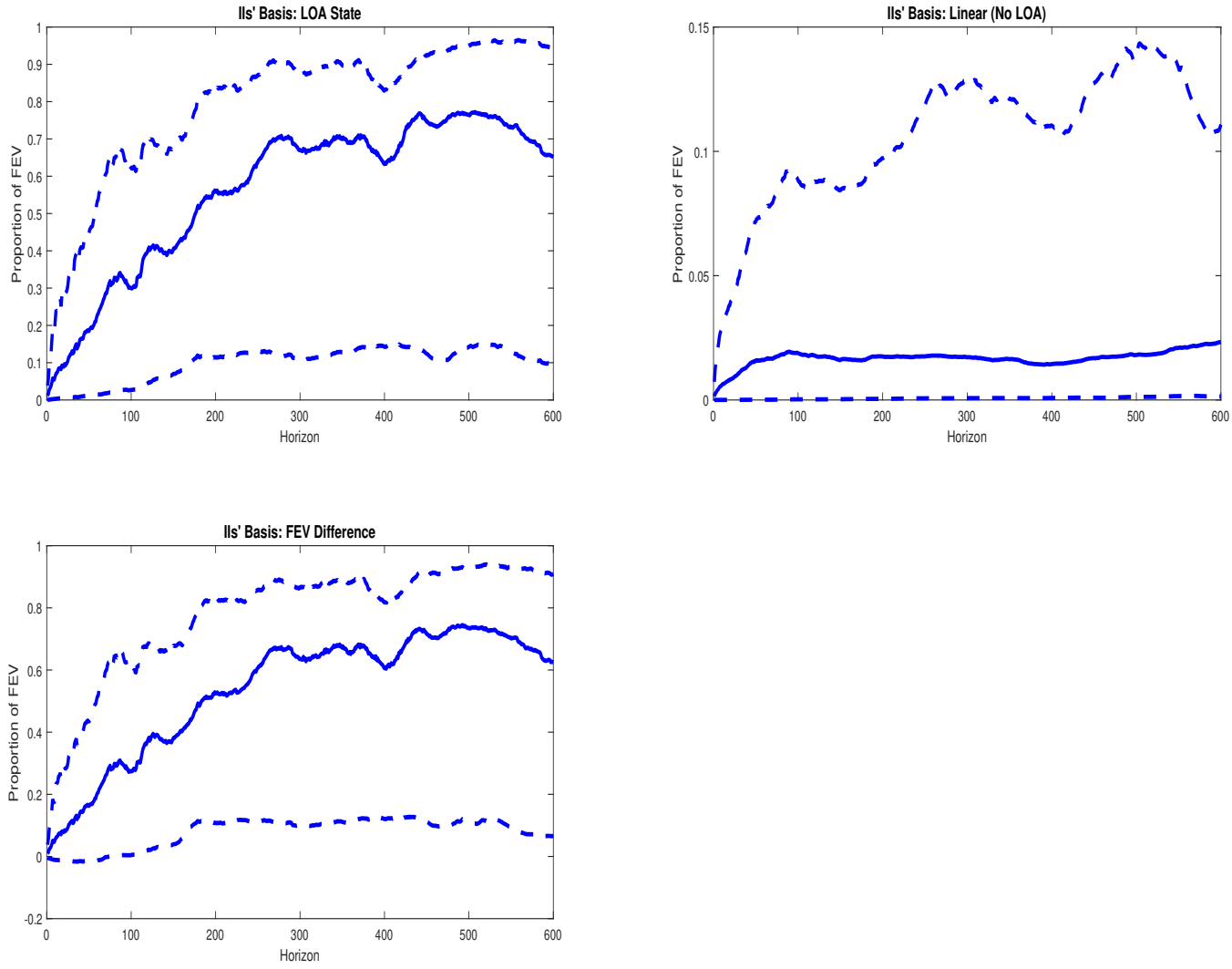

Notes: This figure presents the FEV share of IIs' aggregate cross-currency basis that is attributable to the aggregate FX swap demand shock from the model described by Equations (14) and (15) from the text, where now the sample is truncated at February 28, 2020 so as to exclude the COVID-ridden period. The first and second columns show the FEV contributions in the LOA state and linear (no LOA) case, respectively; and the third column shows the FEV contribution differences across these two cases. Horizon (on the x-axis) is in days and the FEV share is on the y-axis.

Figure B.6: **LOA-Dependent Impulse Responses of IIs' Aggregate Open FX Swap Position to a One Standard Deviation Aggregate FX Swap Demand Shock: Excluding COVID**.

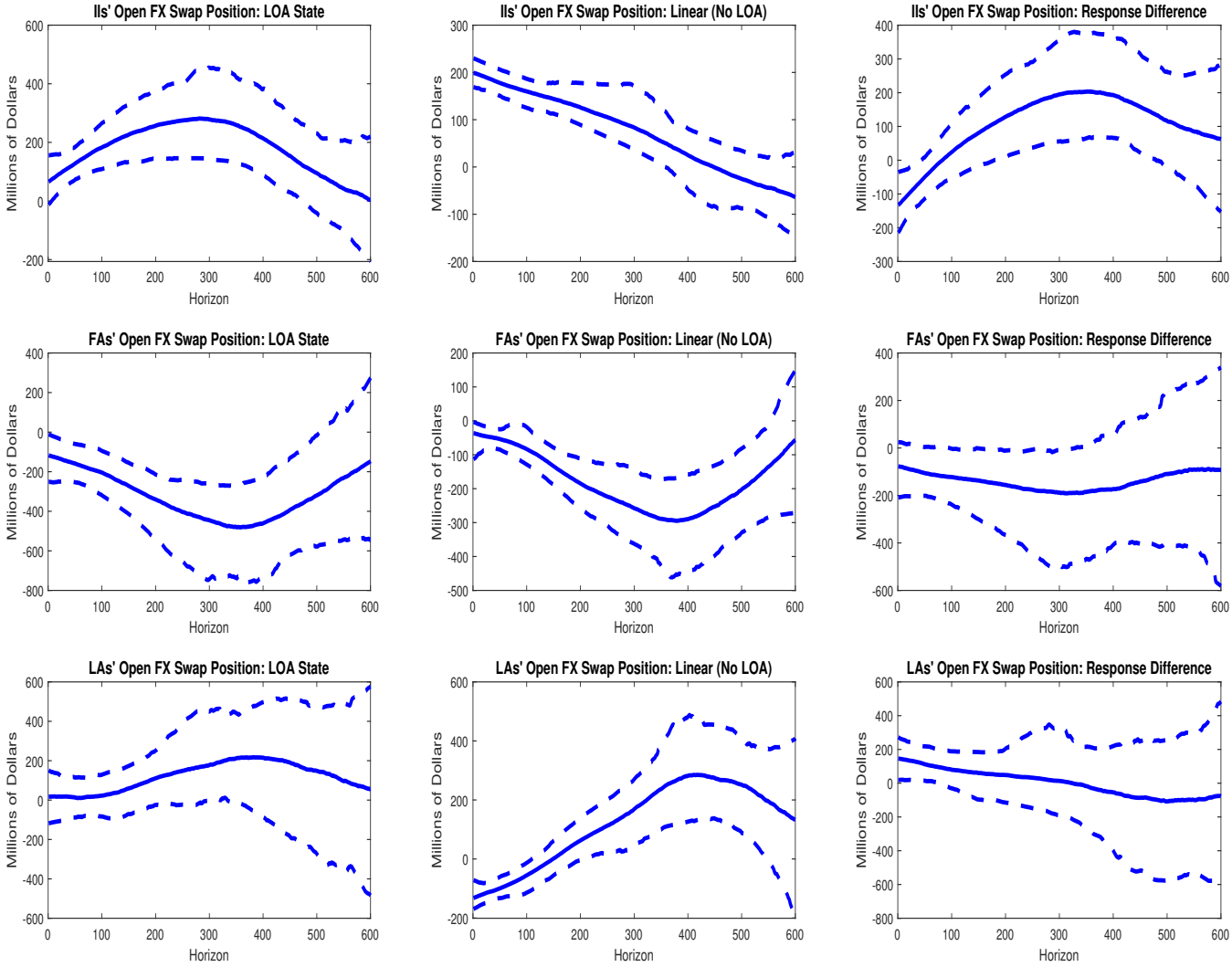

Notes: This figure presents the LOA-dependent impulse responses of IIs', local arbitrageurs' (LAs'), and foreign arbitrageurs' (FAs') aggregate open swap positions to a one standard deviation aggregate FX swap demand shock from the model described by Equations (14) and (15) from the text where the outcome variable in the latter equation (accumulated difference in IIs' basis) is now replaced by the accumulated difference in the corresponding sector's open FX swap position (i.e., $SP_{t+h,j} - SP_{t-1,j}$, where $j = [IIs, LAs, FAs]$). Different from the baseline case, the sample is truncated at February 28, 2020 so as the exclude the COVID-ridden period. The first and second columns show the responses in the LOA state and linear (no LOA) case, respectively; and the third column shows the response differences across these two cases. Responses are in terms of deviations from pre-shock values (in millions of dollars terms). Horizon (on x-axis) is in days.

Figure B.7: **LOA-Dependent Impulse Responses of IIs' Aggregate Cross-Currency Basis to a One Standard Deviation Aggregate FX Swap Demand Shock: Increasing Lags in Micro Regressions**.

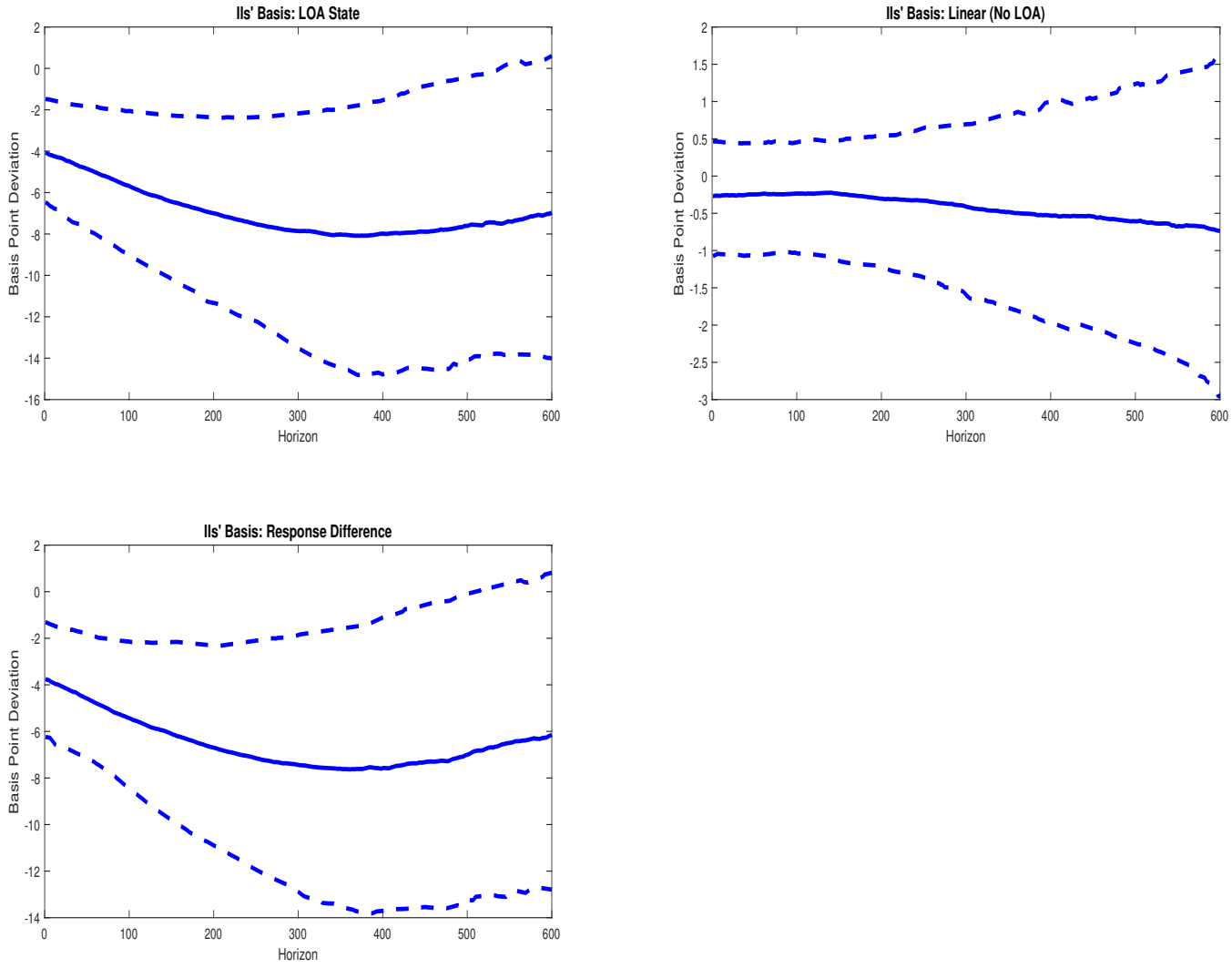

Notes: This figure presents the LOA-dependent impulse responses of IIs' aggregate cross currency basis to a one standard deviation aggregate FX swap demand shock from the model described by Equations (14) and (15) from the text, where now the lags in the micro II-level regressions underlying the former equation are based only on the corrected AIC test. The first and second columns show the responses in the LOA state and linear (no LOA) case, respectively; and the third column shows the response differences across these two cases. Responses are in terms of deviations from pre-shock values (basis point deviations). Horizon (on x-axis) is in days.

Figure B.8: **LOA-Dependent FEV Shares of IIs' Aggregate Cross-Currency Basis Attributable to the Aggregate FX Swap Demand Shock: Alternative LOA Measure: Increasing Lags in Micro Regressions**.

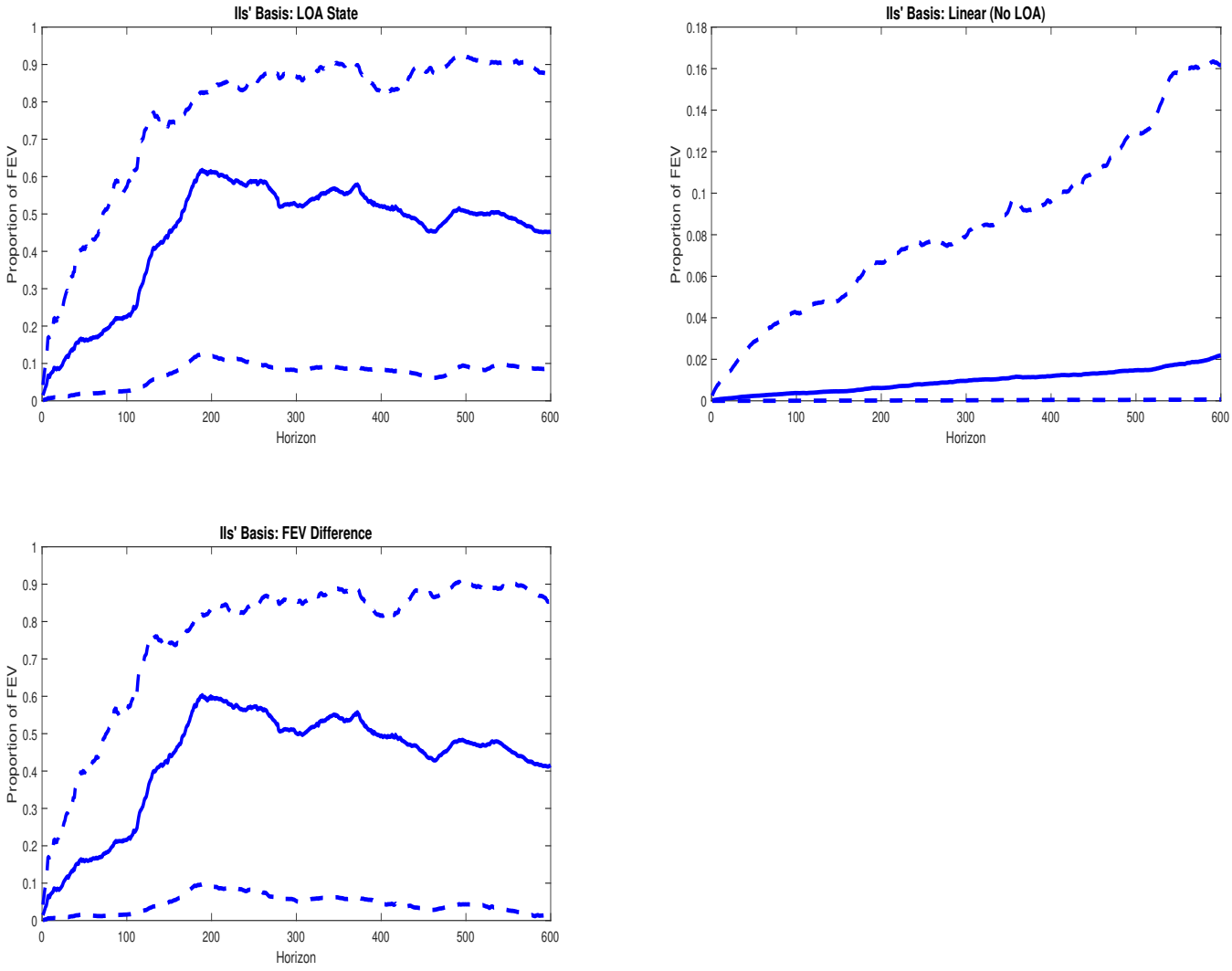

Notes: This figure presents the FEV share of IIs' aggregate cross-currency basis that is attributable to the aggregate FX swap demand shock from the model described by Equations (14) and (15) from the text, where now the lags in the micro II-level regressions underlying the former equation are based only on the corrected AIC test. The first and second columns show the FEV contributions in the LOA state and linear (no LOA) case, respectively; and the third column shows the FEV contribution differences across these two cases. Horizon (on the x-axis) is in days and the FEV share is on the y-axis.

Figure B.9: **LOA-Dependent Impulse Responses of IIs' Aggregate Open FX Swap Position to a One Standard Deviation Aggregate FX Swap Demand Shock: Increasing Lags in Micro Regressions**.

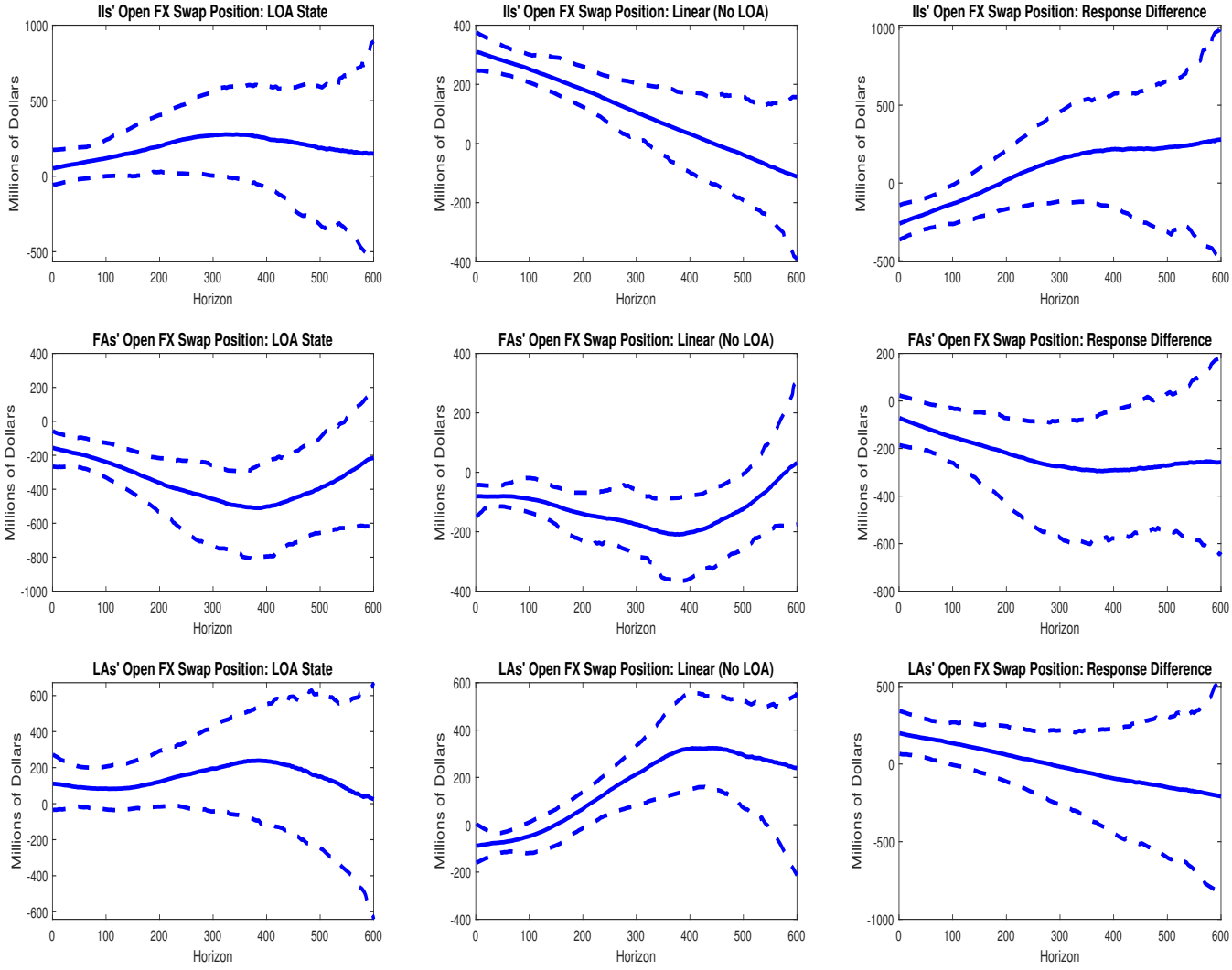

Notes: This figure presents the LOA-dependent impulse responses of IIs', local arbitrageurs' (LAs'), and foreign arbitrageurs' (FAs') aggregate open swap positions to a one standard deviation aggregate FX swap demand shock from the model described by Equations (14) and (15) from the text where the outcome variable in the latter equation (accumulated difference in IIs' basis) is now replaced by the accumulated difference in the corresponding sector's open FX swap position (i.e., $SP_{t+h,j} - SP_{t-1,j}$, where $j = [IIs, LAs, FAs]$). Different from the baseline case, the lags in the micro II-level regressions underlying Equation (14) from the text are based only on the corrected AIC test. The first and second columns show the responses in the LOA state and linear (no LOA) case, respectively; and the third column shows the response differences across these two cases. Responses are in terms of deviations from pre-shock values (in millions of dollars terms). Horizon (on x-axis) is in days.

References

Barnichon, R. and Brownlees, C.: 2019, Impulse Response Estimation by Smooth Local Projections, *The Review of Economics and Statistics* **101**(3), 522–530.

Cornea-Madeira, A.: 2017, The Explicit Formula for the Hodrick-Prescott Filter in a Finite Sample, *The Review of Economics and Statistics* **99**(2), 314–318.

Giannone, D., Lenza, M. and Primiceri, G. E.: 2015, Prior Selection for Vector Autoregressions, *The Review of Economics and Statistics* **97**(2), 436–451.

Gómez, V.: 1999, Three equivalent methods for filtering finite nonstationary time series, *Journal of Business & Economic Statistics* **17**(1), 109–116.

Hamilton, J. D.: 2018, Why You Should Never Use the Hodrick-Prescott Filter, *The Review of Economics and Statistics* **100**(5), 831–843.

Harvey, A. C.: 1990, *Forecasting, Structural Time Series Models and the Kalman Filter*, Cambridge University Press.

He, Z., Kelly, B. and Manela, A.: 2017, Intermediary asset pricing: New evidence from many asset classes, *Journal of Financial Economics* **126**(1), 1–35.

Hodrick, R. and Prescott, E.: 1997, Postwar u.s. business cycles: An empirical investigation, *Journal of Money, Credit and Banking* **29**(1), 1–16.

Miranda-Agrippino, S. and Ricco, G.: 2021, The transmission of monetary policy shocks, *American Economic Journal: Macroeconomics* **13**(3), 74–107.

Müller, U. K.: 2013, Risk of bayesian inference in misspecified models, and the sandwich covariance matrix, *Econometrica* **81**(5), 1805–1849.

Plagborg-Møller, M.: 2016, *Essays in macroeconometrics*, Phd thesis, department of economics, harvard university.

Tanaka, M.: 2019, Bayesian inference of local projections with roughness penalty priors, *Computational Economics* **55**(2), 629–651.

Uhlig, H.: 1994, What macroeconomists should know about unit roots: A bayesian perspective, *Econometric Theory* **10**(3/4), 645–671.